

Effect of a Time Dependent Concrete Modulus of Elasticity on Prestress Losses in Bridge Girders

Brahama P. Singh¹⁾, Nur Yazdani^{2),*}, and Guillermo Ramirez³⁾

(Received November 13, 2012, Accepted March 21, 2013)

Abstract: Prestress losses assumed for bridge girder design and deflection analyses are dependent on the concrete modulus of elasticity (MOE). Most design specifications, such as the American Association of State Highways and Transportation Officials (AASHTO) bridge specifications, contain a constant value for the MOE based on the unit weight of concrete and the concrete compressive strength at 28 days. It has been shown in the past that the concrete MOE varies with the age of concrete. The purpose of this study was to evaluate the effect of a time-dependent and variable MOE on the prestress losses assumed for bridge girder design. For this purpose, three different variable MOE models from the literature were investigated: Dischinger (Der Bauingenieur 47/48(20):563–572, 1939a; Der Bauingenieur 5/6(20):53–63, 1939b; Der Bauingenieur, 21/22(20):286–437, 1939c), American Concrete Institute (ACI) 209 (Tech. Rep. ACI 209R-92, 1992) and CEB-FIP (CEB-FIP Model Code, 2010). A typical bridge layout for the Dallas, Texas, USA, area was assumed herein. A prestressed concrete beam design and analysis program from the Texas Department of Transportation (TxDOT) was utilized to determine the prestress losses. The values of the time dependent MOE and also specific prestress losses from each model were compared. The MOE predictions based on the ACI and the CEB-FIP models were close to each other; in long-term, they approach the constant AASHTO value. Dischinger's model provides for higher MOE values. The elastic shortening and the long term losses from the variable MOE models are lower than that using a constant MOE up to deck casting time. In long term, the variable MOE-based losses approach that from the constant MOE predictions. The Dischinger model would result in more conservative girder design while the ACI and the CEB-FIP models would result in designs more consistent with the AASHTO approach.

Keywords: concrete modulus of elasticity, prestress losses, bridge girders, I-girders.

1. Introduction

The purpose of this study was to examine several existing time dependent moduli of elasticity (MOE) of concrete and evaluate their effect on various prestress losses in typical bridge girders. Towards this end, a method proposed by Dischinger (1939a, b, c) for a variable MOE was considered herein, along with a couple of other methods from the literature. The MOE from Dischinger's method varies with the concrete creep function. The current American Association of State Highways and Transportation Officials (AASHTO) specifications consider the concrete MOE to remain constant through the life of a structure (AASHTO 2010). AASHTO's

calculation of the concrete MOE is based on the unit weight and the 28 day compressive strength of concrete. The two additional methods considered herein were the American Concrete Institute (ACI) 209 Model Code (1992) and CEB-FIP 1990 Model Code (2010). A realistic concrete MOE that varies with concrete age is likely to result in more precise estimation of various prestress losses in concrete girders, resulting in more realistic girder design, prestress estimation, camber calculations and bridge deck design/construction.

Equations for variable MOE of concrete considering types of mineral admixtures and coarse aggregates were developed previously (Nemati 2006). Valuable data and general trends in concrete strengths, creep coefficient and MOE for typical Florida concrete were generated through another study (Tia et al. 2005). Yazdani et al. (2005) developed concrete MOE models based on aggregate classes in Florida and a variable concrete strength. There have been no other studies in the past in which the effects of a variable and time dependent concrete MOE on prestress losses were investigated.

1.1 AASHTO Approach

The AASHTO regulates highway bridge design in the United States. Currently, all bridge design in the state of Texas is performed in accordance with the AASHTO LRFD

¹⁾Bridge Division, Dallas District, Texas Department of Transportation, Mesquite, TX 75150, USA.

²⁾Department of Civil Engineering, University of Texas at Arlington, Arlington, TX 76019, USA.

*Corresponding Author; E-mail: yazdani@uta.edu

³⁾Buildings and Structures, Exponent, Houston, TX 77042, USA.

(Load and Resistance Factor Design) 2007 specifications (TxDOT 2012). The constant MOE of concrete as specified by AASHTO Equation 5.4.2.4-1 (in U.S. units), reproduced in its SI form in Eq. (1).

$$E_c = 0.043 \times w_c^{1.5} \times \sqrt{f'_c} \quad (1)$$

where E_c is the concrete MOE (MPa), w_c is the unit weight of concrete (kg/m^3), and f'_c is the 28 day compressive strength of concrete (MPa).

Equation (1) is valid for concrete with unit weights in the range of $1,442 \text{ kg/m}^3$ (0.90 lbs/ft^3) and $2,483 \text{ kg/m}^3$ (155 lbs/ft^3). The Texas Department of Transportation (TxDOT) considers this equation valid for 28 day compressive strengths up to 58.6 MPa (8.5 ksi) (TxDOT 2005). For the purposes of this work, the unit weight of concrete was taken as $2,403 \text{ kg/m}^3$ (150 lbs/ft^3). The MOE for prestressing strands was taken as 196.5 GPa ($28,500 \text{ ksi}$) per AASHTO LRFD Section 5.4.4.2. AASHTO LRFD Equation 5.9.5.1-1 expresses the prestress loss in girders, as follows:

$$\Delta f_{pT} = \Delta f_{pES} + \Delta f_{pLT} \quad (2)$$

where Δf_{pT} is the total loss, Δf_{pES} is the loss due to elastic shortening, and Δf_{pLT} is the losses due to long-term shrinkage and creep of concrete, and steel relaxation. The loss due to elastic shortening of concrete is given by AASHTO Equation 5.9.5.2.3a-1, as follows:

$$\Delta f_{pES} = \frac{E_p}{E_{ci}} \times f_{cgp} \quad (3)$$

where E_p is the MOE of prestressing steel, E_{ci} is the MOE of concrete at transfer, and f_{cgp} is the sum of concrete stresses at the center of gravity of prestressing tendons due to the prestressing force at transfer and the self-weight of the member at the sections of maximum moment.

The long-term loss is given by AASHTO Equation 5.9.5.3-1, and is reproduced in Eq. (4). In this equation, the first term corresponds to creep loss, the second term to shrinkage loss and the third to relaxation losses.

$$\Delta f_{pLT} = 10.0 \frac{f_{pi} A_{ps}}{A_g} \gamma_h \gamma_{st} + 12.0 \gamma_h \gamma_{st} + \Delta f_{pr} \quad (4)$$

where H is the average annual ambient relative humidity (%)

$$\gamma_h = (1.7 - 0.01H) \quad (\text{AASHTO Eq. 5.9.5.3-2}) \quad (5)$$

$$\gamma_{st} = \frac{5}{1 + f'_{ci}} \quad (\text{AASHTO Eq. 5.9.5.3-3}) \quad (6)$$

f_{pi} is the prestressing steel stress prior to transfer, f'_{ci} is the specified concrete compressive strength at time of prestressing, A_{ps} is the area of prestressing steel, A_g is the gross cross sectional area of girder, γ_h is the correction factor for relative humidity, γ_{st} is the correction factor for specified concrete strength at transfer, and Δf_{pr} is the estimation of relaxation loss, taken as 16.6 MPa (2.4 ksi) for low relaxation strands.

1.2 Dischinger Method

Franz Dischinger (1887–1953) was a well-known German civil and structural engineer who was responsible for the development of the modern cable-stayed bridge. He is known for his work in prestressed concrete and, in 1939, published a theory called “Elastic and Plastic Distortions of Reinforced Concrete Structural Members and in Particular of Arched Bridges” (1939a, b, c). Dischinger showed that the MOE is a function of time since the creep of concrete is also a function of time. Dischinger’s evaluation of the change in concrete MOE with time was based on a creep coefficient determined from laboratory tests. He proposed the following equation for concrete MOE:

$$E_{ot} = E_o(1 + \psi_t) \quad (7)$$

where E_{ot} is the modified MOE at time t , E_o is the initial MOE, and ψ_t is the creep coefficient

AASHTO specifies a concrete creep coefficient (AASHTO Equation 5.4.2.3.2-1), as follows:

$$\psi(t, t_i) = 1.9 k_s k_{hc} k_f k_{td} t_i^{-0.118} \quad (8)$$

where

$$k_s = 1.45 - 0.13 \left(\frac{V}{S} \right) \geq 1.0 \quad \text{AASHTO 5.4.2.3.2-2} \quad (9)$$

$$k_{hc} = 1.56 - 0.008H \quad \text{AASHTO 5.4.2.3.2-3} \quad (10)$$

$$k_f = \frac{5}{1 + f'_{ci}} \quad \text{AASHTO 5.4.2.3.2-4} \quad (11)$$

$$k_{td} = \frac{t}{61 - 4f'_{ci} + t} \quad \text{AASHTO 5.4.2.3.2-4} \quad (12)$$

k_s is the factor for effect of volume to surface ratio, k_f is the factor for the effect of concrete strength, k_{hc} is the humidity factor for creep, k_{td} is the time dependent factor, V/S is the volume to surface ratio, t is the time (days), and t_i is the age of concrete at time of load application (days).

In this study, the creep coefficient from Eq. (8) was calculated and used as the basis for the Dischinger Model (Eq. (7)).

1.3 ACI 209 Method

The ACI 209 Model Code (1992) specifies a time dependent concrete MOE based on a time dependent 28 day compressive strength. The time variable compressive strength (ACI Eq. 2.1) is as follows:

$$f'_c(t) = \frac{t}{a + \beta t} (f'_{c'})_{28} \quad (13)$$

where $f'_c(t)$ is the compressive strength at time t ; t is the time in days; $(f'_{c'})_{28}$ is the 28 day compressive strength; and a and β are constants depending on curing and cement type, respectively.

The values for a and β are reproduced in Table 1. For this study, Type I cement and moist cured concrete were assumed. When girders are manufactured, the concrete is

Table 1 Coefficients from ACI 209 model code.

| | Cement type | | Curing | Duration |
|----------|-------------|------|--------|--------------|
| | I | III | | t_s (days) |
| Strength | | | | |
| a | 4.0 | 2.3 | Moist | |
| | 1.0 | 0.7 | Steam | |
| β | 0.85 | 0.92 | Moist | |
| | 0.95 | 0.98 | Steam | |

normally steam cured to allow for quick turnaround. Both steam and moist curing were checked herein to note the difference in the values for the MOE. The difference in MOE was not significant for either curing type. ACI Equation 20.25 for the variable MOE is given in Eq. (14).

$$E_c(t) = 0.043 \sqrt{w^3 f'_c(t)} \quad (14)$$

where $E_c(t)$ is the MOE of concrete at age t days (MPa), w is the unit weight of concrete (kg/m^3), and $f'_c(t)$ is the compressive strength at time t in days (MPa, Eq. (13)).

1.4 The CEB-FIP Method

The CEB-FIP Model Code (2010) was initially published in 1978 and since then has impacted national codes in many countries. ACI and other well-known codes have referenced the CEB-FIP Code in their publications. The CEB-FIP gives time dependent concrete MOE is given in CEB-FIP Eq. 2.1-57, and presented in the following:

$$E_{ci}(t) = \beta_E(t) E_{ci} \quad (15)$$

where $E_{ci}(t)$ is the concrete MOE at an age of t days, E_{ci} is the concrete MOE at an age of 28 days, and $\beta_E(t)$ is a coefficient depending on the age of concrete (t days); it is given by CEB-FIP Eq. 2.1-58 and is as follows:

$$\beta_E(t) = [\beta_{cc}(t)]^{0.5} \quad (16)$$

where $\beta_{cc}(t)$ is a coefficient depending on the age of concrete (t days), given by CEB-FIP Eq. 2.1-54 and as follows:

$$\beta_{cc}(t) = \exp \left[s \left\{ 1 - \left(\frac{28}{t/t_1} \right)^{0.5} \right\} \right] \quad (17)$$

where t is the age of concrete (days), t_1 is 1 day, s is a coefficient which depends on the type of cement; $s = 0.20$ for rapid hardening high strength cements, 0.25 for normal and rapid hardening cements and 0.38 for slowly hardening cements. In this study, normal hardening cement was assumed. The CEB-FIP Code accounts for maturity of the concrete by allowing the time in days to be adjusted for temperature. In this study, this temperature effect on concrete maturity was not considered. The example bridge location for this study (as described later) was assumed to be in a stable environment with the temperature range per season to remain fairly constant.

2. PSTRS14 Software

The TxDOT developed and maintains the Prestressed Concrete Beam Design and Analysis Program (PSTRS14) (TxDOT 2007). PSTRS14 designs and analyzes standard TxDOT I, TxGirder, Box, U, Double-T, Slab, and non-standard girders (user defined) with low-relaxation or stress-relieved strands. PSTRS14 includes a standard beam section library; however, the user can define unique and non-standard shapes and properties of beams. Furthermore, PSTRS14 assigns default values of material properties. However, the user may also define material properties of beams, slabs, shear keys, and even non-standard composite regions.

PSTRS14 only analyzes and designs simply supported pretensioned concrete beams with draped or straight seven-wire patterns. Straight strands can be debonded; however, draped strands have to be fully bonded. PSTRS14 can simultaneously solve the required strand pattern (including number of required strands), the release and final required concrete strengths. PSTRS14 version 4.2 was used for the study herein. This version designs and analyzes prestressed concrete beams based on AASHTO LRFD Specifications (5th Edition, 2010), AASHTO Standard Specifications for Highway Bridges (17th Edition, 2002), AASHTO Standard Specifications for Highway Bridges (15th Edition, 1994 Interim), American Standard Building Code Requirements for Reinforced Concrete (1989) or the American Railway Engineering Association Specifications (1988).

PSTRS14 is a MS-DOS based system in which a text file is input with material properties, loading and design considerations for a prestressed concrete beam. If values are not entered, the program assumes a set of defaults; however, the user must specify basic information about the beam for the design. This basic information includes the following: beam type (standard name or non-standard), span length (measured center to center of bearing), beam spacing, slab thickness, composite slab width, live load distribution factor, relative humidity, uniform dead load on composite section due to overlay and the uniform dead load on composite section excluding overlay. PSTRS14 allows the user to select the type of output generated. The short summary gives the following information: the number of strands and their eccentricity, draped or bonded strands and how much they are draped or bonded, design stresses, ultimate moment required, camber, dead load deflections due to the slab,

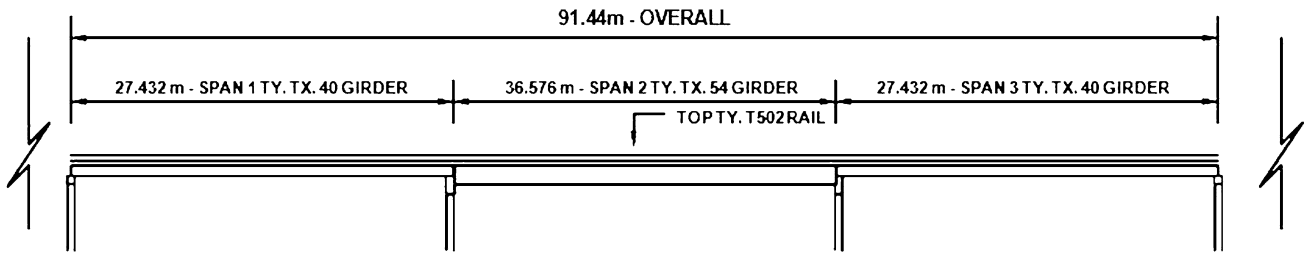


Fig. 1 Profile view of model bridge.

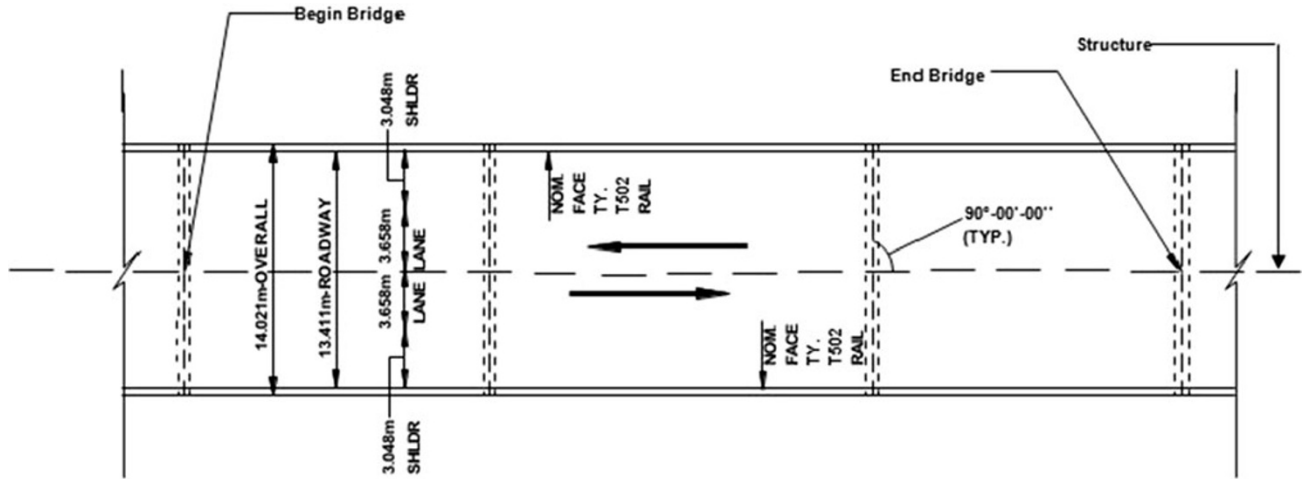


Fig. 2 Plan view of model bridge.

overlay, other loads and the total deflection. For each beam that is to be designed the long format results include moment, shear, stress, and prestress loss tables.

3. Sample Bridge Description

A hypothetical sample bridge was analyzed to evaluate the differences between Dischinger’s modified MOE, the ACI 209 and the CEB-FIP Models for a variable MOE. The typical bridge was assumed to be located in Dallas, Texas, USA with a total length of 91.4 m (300 ft.) and three prestressed spans. As shown in Fig. 1, the bridge consisted of two 27.4 m (90 ft.) spans with Tx-40 girders and one 36.6 m (120 ft.) span with Tx-54 girders, standard shapes used by the TxDOT (2010). A 13.4 m (44 ft.) wide roadway without a skew was modeled. With a 0.3 m (1 ft.) nominal face of rail assumed, an overall width of 13.7 m (46 ft.) was obtained, as shown in Fig. 2. Two 3.7 m (12 ft.) travel lanes and a 3 m (10 ft.) shoulder on each side were assumed. The bridge was modeled with a 200 mm (8 in.) cast in place concrete slab and a 75 mm (3 in.) haunch over the beams. Six girders per span were used at a spacing of 2.4 m (8 ft.) with a 0.9 m (3 ft.) overhang. The bridge cross sections are shown in Fig. 3. A type T502 traffic railing was modeled for this bridge, a standard crash tested TxDOT rail. This railing is applicable for design speeds greater than 80.5 kph (50 miles/h).

3.1 PSTRS14 Software Input

The standard Tx-40 Girder was input into PSTRS14 in two separate designs: as an exterior and an interior girder,

due to different tributary girder spacing. The girder tributary spacing was calculated by Eq. 18 (TxDOT 2012).

$$S_t = \frac{S}{2} + OH \quad (18)$$

where S_t is the effective beam spacing, S is the interior centerline to centerline beam spacing, and OH is the width of overhang of exterior beam.

Using the spacing, the live load distribution factors for moment and shear were calculated and input into PSTRS14. Equation (19) comes from AASHTO 4.6.2.2.2 and calculates the live load distribution factor for moment.

$$LLDF_m = 0.075 + \frac{S^{0.6}}{9.5} \times \frac{S^{0.2}}{L} \times \left(\frac{K_g}{12L t_s^3} \right)^{0.1} \quad (19)$$

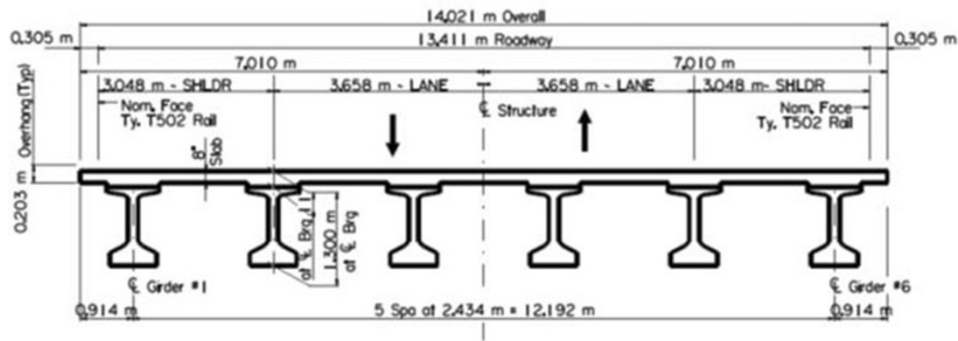
where $LLDF_m$ is the live load distribution factor for moment, S is the beam spacing, L is the length of beam (centerline bearing to centerline bearing), t_s is the slab thickness (in.), and K_g is defined in Eq. (20).

$$K_g = n(I + Ae_g^2) \quad (20)$$

where I is the moment of inertia of the beam (in⁴), A is the area of the beam (in²), e_g is the distance between center of gravity of beam and deck (in.), and n is defined in Eq. (21).

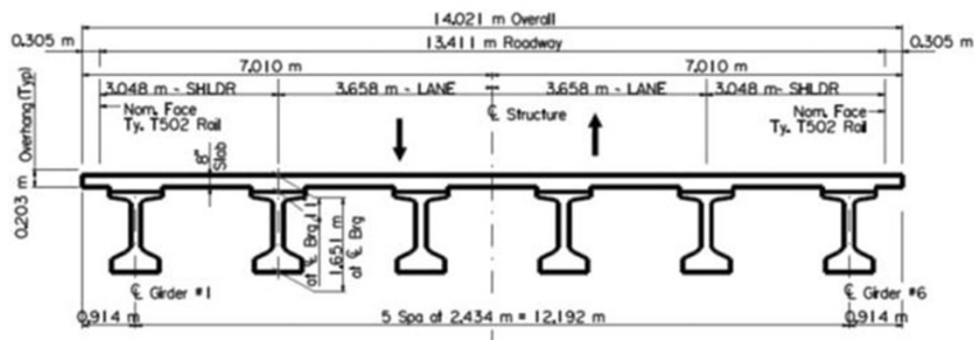
$$n = \frac{E_{beam}}{E_{deck}} \quad (21)$$

where E_{beam} is the MOE of the beam concrete and E_{deck} is the MOE of the deck concrete. For this bridge, the modulus of



TYPICAL TRANSVERSE SECTION
 (SPANS 1 & 3 - TYPE TX, 40 GRIDER)
 N.T.S.

(a) Spans 1 and 3



TYPICAL TRANSVERSE SECTION
 (SPAN 2 - TYPE TX, 54 GRIDER)
 N.T.S.

(b) Span 2

Fig. 3 Bridge cross sections.

Table 2 Girder Information.

| Girder data | Ext. Tx-40 | Int. Tx-40 | Ext. Tx-54 | Int. Tx-54 |
|------------------------|------------|------------|------------|------------|
| C/C bearing length (m) | 26.8 | 26.8 | 36.0 | 36.0 |
| Beam spacing (m) | 2.1 | 2.4 | 2.1 | 2.4 |
| Moment LL dist. factor | 0.585 | 0.643 | 0.579 | 0.636 |
| Shear LL dist. factor | 0.743 | 0.814 | 0.743 | 0.814 |

the beam and deck were assumed to be the same and the value for n was taken as one. The live load distribution factor for shear is defined by AASHTO 4.6.2.2.3 and is given in Eq. (22).

$$LLDF_{shear} = 0.2 + \frac{S}{12} - \left(\frac{S}{3.5}\right)^2 \quad (22)$$

where $LLDF_{shear}$ is the live load distribution factor for shear and S is the beam spacing (ft.).

Table 2 summarizes the input data for each of girder type. AASHTO Fig. 5.4.2.3.3-1 gives the annual average ambient relative humidity in percent. The percentage relative humidity was taken as 65 %, the average humidity encountered in Dallas, Texas, in a year, as per AASHTO

recommendations. Per TxDOT standards, TxDOT class H concrete was assumed with a minimum 28 day compressive strength of 27.6 MPa (4 ksi). TxDOT also assumes a constant concrete MOE of 34.5 GPa (5 ksi), the steel MOE of 196.5 GPa (29,000 ksi), unit weight of concrete of 2,403 kg/m³ (150 lb/ft³) and prefers the use of 12 mm (0.5 in.) low relaxation prestressing strands with a tensile strength of 1,862 MPa and yield strength of 414 MPa (TxDOT 2004).

4. Moe Analysis and Results

The values of the time dependent MOE for CEB-FIP, ACI and Dischinger methods were compared herein, using the PSTRS14 as the calculation tool. The coefficient of creep

Table 3 Construction time intervals used for MOE analysis.

| t_{final} (days) | Description |
|--------------------|-----------------------------|
| 2 | Initial stress transfer |
| 10 | Girder curing |
| 14 | Girder placement at jobsite |
| 104 | Casting of deck on girders |
| 134 | Casting of railing |
| 254 | Bridge opening to traffic |
| 365 | At 1 year |
| 730 | At 2 years |

Table 4 MOE calculation parameters during construction time intervals.

| t_{final} (days) | k_c [Eq. (11)] | Creep coefficient, ψ [Eq. (9)] | ACI $f'_c(t)$, MPa [Eq. (12)] |
|--------------------|------------------|-------------------------------------|--------------------------------|
| 2 | 0.149 | 0.04 | 1,404 |
| 10 | 0.169 | 0.15 | 3,200 |
| 14 | 0.178 | 0.18 | 3,522 |
| 104 | 0.327 | 0.66 | 4,502 |
| 134 | 0.360 | 0.77 | 4,546 |
| 254 | 0.451 | 1.08 | 4,620 |
| 365 | 0.502 | 1.27 | 4,646 |
| 730 | 0.586 | 1.60 | 4,676 |

used in Dischinger's MOE model was assumed to be the same for the Tx-40 and Tx-54 girders since the volume to surface area ratio variation in Eq. (9) can be a maximum of 152 mm (6 in.) per AASHTO 5.4.2.3.2. This upper limit controlled for both girder types. The constants a and β (Table 1) were assumed as 4 and 0.85, respectively. The concrete strength factor k_f (Eq. (11)) was found to be 0.8973.

The girders were analyzed for time intervals representing various stages of construction (Table 3). The time was measured from the day the girder was cast (day 1). Per TxDOT standard specifications, the girder must be cured for a minimum of 10 days. Once a girder is cured and passes the inspection processes, it is typically shipped directly to the jobsite or stored at the yard. It was assumed herein that after curing, it is shipped to the jobsite within 4 days. It is difficult to evaluate when construction loads/permanent dead loads (of the deck) are placed on the girder since each project and contractor schedule are different. For this analysis, a time frame of 3 months was assumed until the deck was cast and another 1 month until the railing was placed. This bridge was assumed to be open to traffic 4 months after the railing was cast. Table 4 gives various calculated parameters for MOE calculation for these time intervals. In order to further analyze long-term MOEs, longer time frames of 1, 2, 5 years and up to 50 years (assumed life of bridge) were also investigated. The corresponding calculated MOE parameters are presented in Table 5.

Plots of the calculated MOE values for various construction time sequences and longer time frames are presented in Figs. 4 and 5, respectively. It can be seen from Fig. 4 that the MOE from the ACI 209 and the CEB-FIP Models are in close agreement. These values become almost constant after the time interval assumed for the deck casting (104 days). Furthermore, the ACI and the CEB-FIP values reach a maximum MOE of around 37 GPa (5,387 ksi), which is close to the constant value used by TxDOT (34.4 GPa or 5,000 ksi). Dischinger's proposed method for the MOE shows significantly higher values, as compared to ACI and CEB-FIP models, and continues to increase for the duration of the construction period. This significant difference may be attributed to the nature of the Dischinger's model (Eq. (7)). This equation depends linearly on the creep coefficient and increases as the creep coefficient increases. Because the creep coefficient is linearly dependent upon time (Eq. (8)), the Dischinger equation yields MOE values that are time dependent. As seen in Eqs. (14) and (15), the MOE values from the ACI 209 and the CEB-FIP models are functions of the square root of the time-dependent concrete compressive strength. So, unlike the CEB-FIP and the ACI 209 Method predictions, the Dischinger Method continues to show a significant increase in MOE after the deck casting. Figure 5 shows that the MOE from the ACI and the CEB-FIP models remain almost constant throughout the service life. However, the values predicted by Dischinger Model increases slightly,

Table 5 MOE calculation parameters for 5–50 years.

| t_{final} (years) | k_c (Eq. 11) | Creep coefficient, ψ (Eq. 8) | ACI $f'_c(t)$, MPa (Eq. 13) |
|----------------------------|----------------|-----------------------------------|------------------------------|
| 5 | 0.659 | 1.94 | 4,698 |
| 10 | 0.689 | 2.09 | 4,700 |
| 15 | 0.700 | 2.16 | 4,702 |
| 20 | 0.705 | 2.19 | 4,703 |
| 25 | 0.709 | 2.22 | 4,703 |
| 30 | 0.711 | 2.23 | 4,704 |
| 35 | 0.713 | 2.25 | 4,704 |
| 40 | 0.714 | 2.26 | 4,704 |
| 45 | 0.715 | 2.26 | 4,704 |
| 50 | 0.716 | 2.27 | 4,705 |

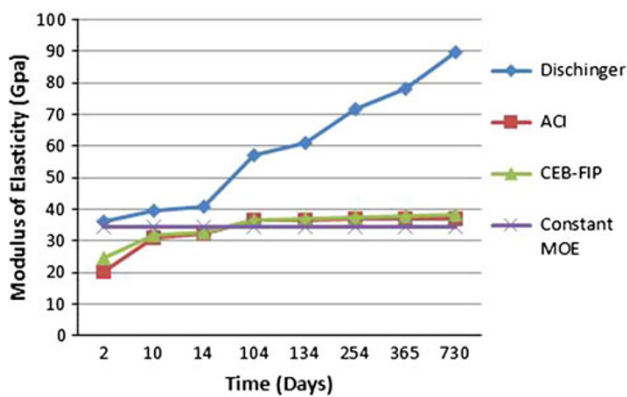


Fig. 4 Variation of MOE for construction time intervals.

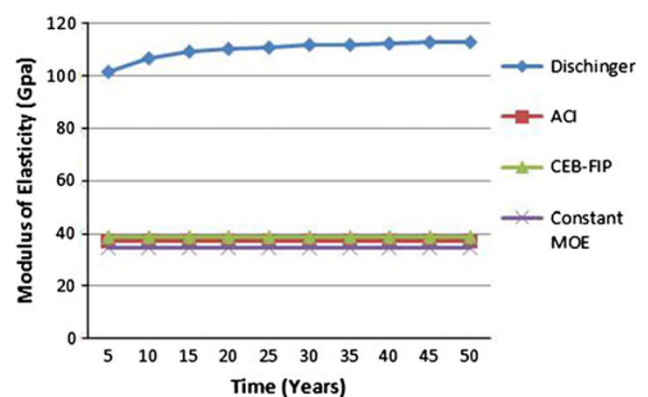


Fig. 5 Variation of MOE from 5 to 50 years.

yet remain fairly close to approximately 110 GPa (16,000 ksi).

4.1 Effects of Variable MOE on Prestress Losses During Construction

The PSTRS14 summary output contained predicted values of different types of prestress losses, percentage of losses at release and a final value. In this study, the effect of variable MOE was investigated on elastic shortening and creep losses during the construction time sequences. Since the relative humidity was taken to be constant, the effect on shrinkage losses was not evaluated.

The dead load due to overlay and railing was input into PSTRS14. Other loads included the dead load of the slab and the live load. The live load was automatically calculated by PSTRS14 based on the AASHTO LRFD specifications. For this study, a 50 mm (2 in.) overlay thickness was assumed. TxDOT calculates this uniform dead load due to overlay as 37 kg/m (0.025 kip/ft). To determine the load per girder, this dead load was multiplied by the beam spacing, as shown in Eq. 23.

$$DL_{\text{overlay}} = DL \times S \quad (23)$$

where DL_{overlay} is the uniform dead load due to overlay per girder, DL is the uniform dead load due to overlay, and S is the beam spacing (varies for interior and exterior girders)

Table 6 Dead load for girders (kg/m).

| Load | Exterior girder | Interior girder |
|----------------|-----------------|-----------------|
| Due to overlay | 260 | 298 |
| Due to railing | 155 | 155 |

For exterior girders, the tributary spacing was used to calculate the dead load. In the case of this model bridge, no sidewalks or temporary railings were assumed. From the TxDOT bridge railing standards (TxDOT 2012), the uniform dead load for the railing was found as 466 kg/m (0.313 kip/ft). To find the dead load per girder, the total uniform dead load from both rails was divided by the number of girders in the span. In the model bridge, the number of beams in all spans was the same, resulting in identical dead loads. Table 6 gives the values for the superimposed dead loads. A default value for the live load impact factor of 1.33 was assumed by the software for the HL-93 live load from AASHTO.

The elastic shortening loss results from PSTRS14 with the variable MOE inputs for the Tx-40 exterior and interior girders are shown in Figs. 6 and 7. As seen in Eq. 7, the Dischinger MOE model is only dependent on the initial concrete compressive strength (linearly), while the ACI 209

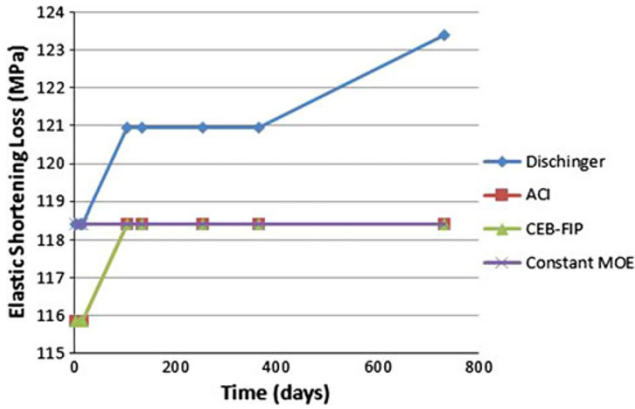


Fig. 6 Elastic shortening loss for Tx-40 exterior girder.

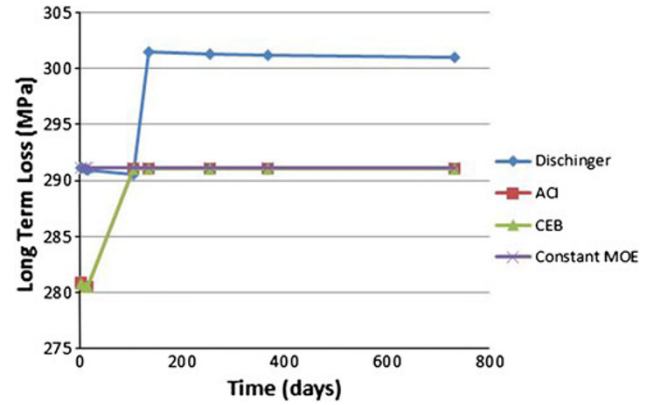


Fig. 9 Long term loss for Tx-40 interior girder.

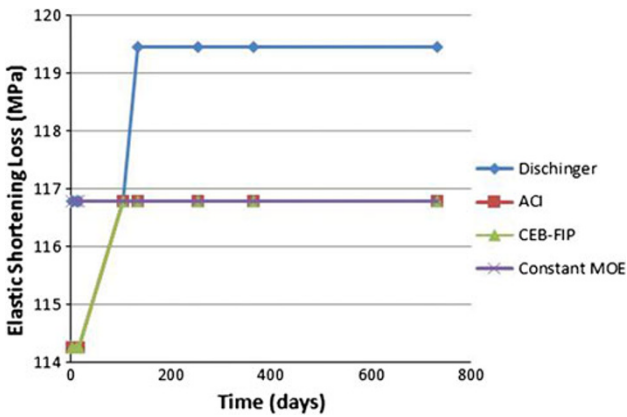


Fig. 7 Elastic shortening loss for Tx-40 interior girder.

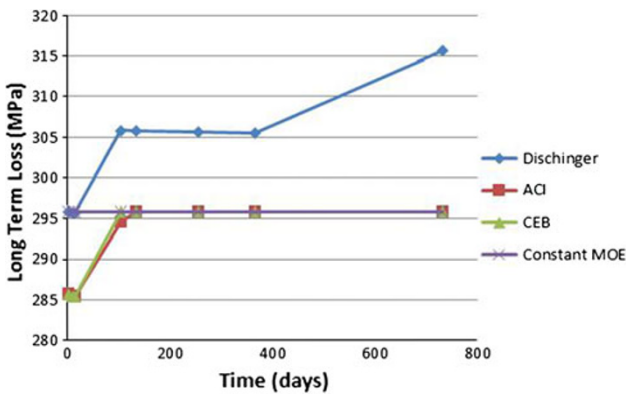


Fig. 8 Long term loss for Tx-40 exterior girder.

MOE model is a function (square root) of the time-dependent concrete compressive strength. In the CEB-FIP model, there is no direct effect of the concrete compressive strength. Equation (3) shows that the elastic shortening loss is dependent on the concrete stresses at the center of the prestressing tendons due to prestressing force (varies with time) and self-weight. Therefore, there was an increase in the Dischinger elastic shortening losses at 104 and 730 days (2 years) for the exterior girders. This can be attributed to the number of prestressing strands necessary to meet design requirements. PSTRS14 output showed that stresses, strands and eccentricity of the strands all increased at these time frames. The resulting increase of the concrete fiber stress at the steel

center of gravity at transfer caused increase in the elastic shortening loss. The CEB-FIP and the ACI 209 losses are in agreement since the MOE values are approximately equal. The elastic shortening loss remained constant after 104 days when the value for MOE becomes constant in these two methods. Furthermore, the CEB-FIP and ACI models produced elastic shortening losses that are predicted by a constant MOE value. The interior girder shows an increase in the elastic shortening loss around 104 days with the Dischinger MOE. From the detailed PSTRS14 design report it was found that the stresses, strands and eccentricity of the strands increase in these time periods for the girder. Contrary to what was seen with the exterior girders, the interior girders were more stable for elastic shortening losses.

The long term loss behavior (Eq. (4)) with variable time-dependent MOE is similar to the behavior of elastic shortening loss. Figures 8 and 9 present the total long term loss predictions (Eq. (4)) for the TxDOT exterior and interior girders. The plots have similar variations as the elastic shortening loss plot; however, the magnitude of the losses is different. This similarity is due to the fact that the creep loss part of Eq. (4) is also dependent upon the concrete stress at the center of gravity of the prestressing steel at transfer. Similar behavior of interior and exterior girders and between the Tx-40 and the Tx-54 girders were observed.

4.2 Long-Term Effects of a Variable MOE on Prestress Loss

The prestress losses calculated by the PSTRS 14 software were also analyzed for a period of 5–50 years at 5 year intervals. Once again, the Dischinger Method predicted losses higher than the CEB-FIP and ACI 209 Models. However, it was noticed that, with the Dischinger Method, the long term losses all reached a maximum at 5 years and then remained constant for the service life. With the exception of the interior Tx-54 girder, the other three types of girders exhibited this behavior. The Tx-54 interior girder attained its maximum losses at 10 years. This girder was the longest and carried the maximum load of the four girders used. It showed an increase in the number of prestressing strands necessary at 10 years; therefore, this result is expected. The CEB-FIP and ACI Models both showed constant losses in these time intervals.

5. Conclusions

The following conclusions may be made based on the findings from this study:

1. The time dependent concrete MOE predicted by the ACI 209 and the CEB-FIP models are in close agreement for short term as well as long term situations. These values become approximately constant after the deck casting at 104 days. The predictions from the two models approach the constant MOE value recommended by AASHTO and TxDOT specifications (34.4 GPa).
2. At initial conditions (less than 14 days after casting), the code specified constant MOE is greater than the MOEs predicted by ACI and CEB-FIP. At 2 days, the difference is almost 55 %.
3. The MOEs from the ACI and the CEB-FIP models result in elastic shortening losses that were less than that resulting from the constant MOE up to 104 days after casting. However, the differences are small (around 4 %). After this time, the elastic shortening losses approached the constant value. The Dischinger prediction for this loss was slightly higher. Similar trends were noted for exterior and interior girders.
4. The variations in the long term losses were similar to that for the elastic shortening losses. This similarity is due to the fact that both loss types are dependent on the concrete stress at the center of gravity of the prestressing steel at transfer.
5. The use of Dischinger's method would produce a more conservative beam design in general, as opposed to that for the constant or the ACI/CEB-FIP models.
6. Dischinger's method provides a simple approach for the calculation of a variable MOE. However, the ACI and the CEB-FIP methods produce MOE and prestress loss values that are in close agreement with each other. They are also in line with the constant MOE and the resulting losses for concrete bridge I-girders.

Open Access

This article is distributed under the terms of the Creative Commons Attribution License which permits any use, distribution, and reproduction in any medium, provided the original author(s) and the source are credited.

References

- American Association of State Highway and Transportation Officials (AASHTO). (2010). *AASHTO LRFD Bridge Design Specifications*. 5th Edition, Washington DC, USA.
- American Concrete Institute (ACI). (1992). *Prediction of creep, shrinkage, and temperature effects in concrete structures*. Technical Publication. ACI 209R-92.
- CEB-FIP. (2010). *CEB-FIP Model Code 2010*. Comité Euro-International du Béton.
- Dischinger, F. (1939a). Elastische und Plastische Verformungen Der Eisenbetontragwerke Und Insbesondere Der Bogenbrücken. *Der Bauingenieur*, 47/48 (20), 563–572.
- Dischinger, F. (1939b). Elastische und Plastische Verformungen Der Eisenbetontragwerke Und Insbesondere Der Bogenbrücken. *Der Bauingenieur*, 5/6 (20), 53–63.
- Dischinger, F. (1939c). Elastische und Plastische Verformungen Der Eisenbetontragwerke Und Insbesondere Der Bogenbrücken. *Der Bauingenieur*, 21/22 (20), 286–437.
- Nemati, K. M. (2006). *Modulus of elasticity of high-strength concrete*. Karachi: CBM-CI International Workshop.
- Texas Department of Transportation (TxDOT). (2004). *Texas Department of Transportation standard specifications*. Austin: Texas Department of Transportation.
- Texas Department of Transportation (TxDOT). (2005). *LRFD bridge design manual*. Austin: Texas Department of Transportation.
- Texas Department of Transportation (TxDOT). (2007). *Prestressed concrete beam design/analysis program user guide*. Austin: Texas Department of Transportation.
- Texas Department of Transportation (TxDOT). (2010). *Bridge design standards*. Austin: Texas Department of Transportation.
- Texas Department of Transportation (TxDOT). (2012). *Bridge railing manual*. Austin: Texas Department of Transportation.
- Tia, M., Liu, Y., & Brown, D. (2005). Modulus of elasticity, creep and shrinkage of concrete. Final report, Florida Department of Transportation, Contract No. BC-354.
- Yazdani, N., McKinnie, B., & Haroon, S. (2005). Aggregate based modulus of elasticity for Florida concrete. *Journal of Transportation Research Record (TRR)*, 1914, 15–23.